# Biosensing using long-range surface plasmon structures

Carlos G. Martínez-Arias, Marco A. Escobar, J. R. Guzman-Sepulveda, Miguel Torres-Cisneros, Rafael Guzman-Cabrera

Carlos G. Martínez-Arias, Marco A. Escobar, J. R. Guzman-Sepulveda, Miguel Torres-Cisneros, Rafael Guzman-Cabrera, "Biosensing using long-range surface plasmon structures ," Proc. SPIE 10728, Biosensing and Nanomedicine XI, 107280F (5 September 2018); doi: 10.1117/12.2320281

Event: SPIE Nanoscience + Engineering, 2018, San Diego, California, United States

# Biosensing using long-range surface plasmon structures

Carlos G. Martínez-Arias[a], Marco A. Escobar[b], J. R. Guzman-Sepulveda[c],
Miguel Torres-Cisneros[a], Rafael Guzman-Cabrera[a]

[a]Universidad de Guanajuato, km 3.5 + 1.8 road Salamanca-Valle de Santiago, Salamanca, Guanajuato, MEX, 36730.
[b]Universidad de la Salle Bajio, Av. Universidad 602, Col. Lomas del Campestre, Leon, Guanajuato, MEX, 36700.
[c]CREOL, The College of Optics and Photonics, University of Central Florida, 4304 Scorpius St., Orlando, FL, USA

## ABSTRACT

We report a parametric study of a long-range plasmon waveguide for the modal profiles, effective index and propagation losses as a function of the metal layer thickness and the variations in the refraction index of the upper cladding. Such device can be used as an optical biosensor. All calculations are performed using COMSOL Multiphysics, and the amplitude- and phase- responses of the device are obtained from the changes in the real and imaginary part of the effective index of the plasmon mode, respectively.

**Keywords:** LRSPP, single-interface SPP, effective index, normalized attenuation, propagation length.

## 1. INTRODUCTION

A biosensor is a device that uses specific biochemical reactions mediated by isolated enzymes, immunesystems, tissues, organelles or whole cells to detect chemical compounds usually by electrical, thermal or optical signals[1]. Although there are several methods for the detection of biomolecules, optical biosensors have the advantages that the duration of the tests can be significantly reduced, no biomolecular labels are required, and the test sample volumes can be minimized[2,3].

Surface plasmon polaritons (SPPs) are transverse magnetic (TM) polarized optical surface waves that propagate, typically, along a metal-dielectric interface[4–6]. The SPP phenomenon was proposed as an immunosensor in 1983 by Liedberg et. al.[7]. Since then, the use of this technology for biodetection has increased significantly, especially in the pharmaceutical industry[8,9]. Although the SPPs have been successfully applied to optical biodetection, the high attenuation of the propagation modes make their use unpractical when long propagation lengths are required, thus limiting the scope of SPP devices application[6].

The long-range SPPs (LRSPP) differentiate from single-interface SPP in the geometrical configuration. The metal strip is much thinner, around a few nanometers, and it is surrounded by dielectric materials with low refractive index contrast. These differences mitigate the problems of high attenuation and short propagation length that are present in the single-interface SPP[6]. While the propagation length of single-interface SPPs is a few microns, the propagation length in the LRSPP can be extended to millimeters[10]. Consequently, a larger detection area is created, improving sensitivity, but a negative consequence of this modification is the loss of confinement of the propagating mode[10]. The LRSPP can be excited by directly butt-coupling an optical fiber to the plasmonic waveguide, which allows for the miniaturization of the device[9,11]. The sensitivity of LRSPP-based devices is very high to refractive index changes in the dielectrics around the metallic strip. In biosensor design, it is important to choose a dielectric that has a refractive index close to the refractive index of the biologically compatible fluids[10,11]. Because analytes usually have a refractive index close to that of the water (~1.33), it is advisable to use dielectrics as Cytop, since this material has an index of refraction of 1.34[12,13]. The optical symmetry around the metal layer can be preserved without major alterations.

We perform a parametric study of a biosensor geometry in two parts. In the first part, we vary the thinckenss of the metal strip from 5 nm to 40 nm, and the real and imaginary parts of the effective refraction index of the fundamental modes are obtained. In the second part, the metal thickness is set, and a multilayer structure is used, then the index of refraction of the upper cladding is varied from 1.33 to 1.34, in intervals of 0.0005, and the real and imaginary parts of the effective index of the plasmonic mode are calculated once more.

Biosensing and Nanomedicine XI, edited by Hooman Mohseni, Massoud H. Agahi,
Manijeh Razeghi, Proc. of SPIE Vol. 10728, 107280F · © 2018 SPIE
CCC code: 0277-786X/18/$18 · doi: 10.1117/12.2320281

## 2. LONG-RANGE SURFACE PLASMON POLARITON WAVEGUIDE

In Fig. 1(a) a diagram of a plasmonic straight waveguide is shown, this structure is formed by an Au film, $\varepsilon_r = -132 + 12.65j$ corresponding to an operating wavelength $\lambda_0 = 1550nm$ [15], embedded into Cytop, $n_1 = 1.34$. The frontal cross-section of the device geometry is formed by two concentric rectangles, and the SPP is excited into the waveguide by a polarized electromagnetic wave (TM). The initial geometric parameters of the metal film are a thickness of 5 nm and a width of 5 $\mu m$. In a first computational analysis, the thickness of the metal is varied from 5 nm to 40 nm in 5 nm increments, in experiments by Krupin et. al.[11] a straight waveguide of a 35 nm thickness was used. In Fig. 1(b) the LRSPP propagation mode along the metal strip is shown, it can be noted that the field distribution is symmetrical, with this configuration the propagation length of the device can reach up to 2 mm length. Therefore, the detection area of a biosensor will increase significantly in comparison to single-interface SPP devices[6,11].

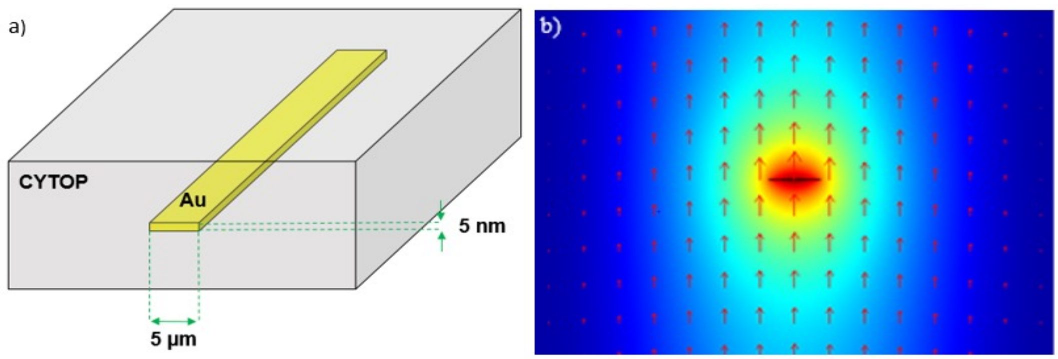


Figure 1. a) Front cross-sectional sketch of symmetric LRSPP waveguide biosensor, b) COMSOL geometry construction.

In Fig. 2(a) a multilayer structure LRSPP is presented, the structure consists of a metal strip of Au embedded between two rectangular boxes, 50 $\mu m$ width by 10 $\mu m$ height each one, the lower one represents the Cytop dielectric and the upper the analyte that will take the optical characteristics of the biological fluids[10,14]. The geometric parameters of the metal strip were determined by our first analysis to 5 $\mu m$ width and a 30 nm thickness.

The LRSPP attenuation was calculated as a function of the changes in the refractive index of the upper box, $n_3$, from $1.33 - 1.34$ in 0.0005 increments. The complex effective index is composed of the effective index $n_{eff}$ (real part) and the normalized attenuation (imaginary part), the propagation length $L_p$ is computed as

$$L_p = \frac{1}{2\alpha} \tag{1}$$

The propagation length corresponds to distance where the intensity of SPP has decreased by a factor of $1/e$, and $\alpha$ is the attenuation of the plasmon mode. The attenuation constant relates to the normalized attenuation $k_{eff}$ by means of the wave number $k_o$, $\alpha = k_{eff} k_o$ [4]. By obtaining the attenuation of the propagating wave, the optical power output of the system can be calculated, and consequently the concentration of biological entities can be estimated.

The cross-sectional geometry and the fundamental mode are shown in Fig. 2 (b), in the second computational analysis, the goal is to calculate the dispersion of the real and imaginary parts of the surface plasmon effective index as a function of the change of the refractive index of the upper box of the LRSPP multilayer structure.

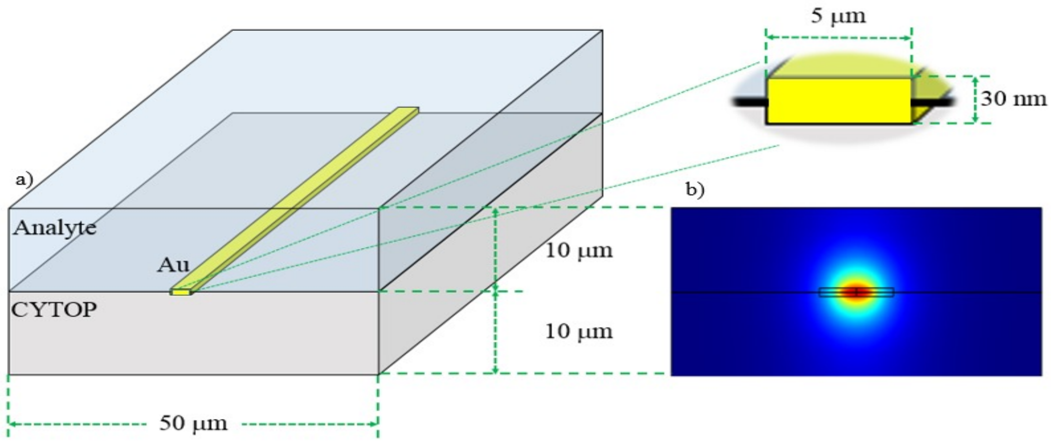


Figure 2. a) complete geometry diagram of LRSPP multi-layer waveguide biosensor, b) COMSOL geometry construction.

## 3. RESULTS AND DISCUSSION

The calculated propagation modes can be observed in Fig. 3. In Fig. 3(a) the propagation mode for metal strip of 5 nm thickness is shown, it can be observed that the field distribution is symmetric and that the electromagnetic confinement is very different from Fig. 3(h) where the propagation mode for a metal strip of 40 nm thickness is shown. From Fig. 3, it is possible to observe that as the metal thickness is increased, Fig. 5 b, c, d, the electromagnetic confinement increases. However, as it can be inferred from Table 1 the propagation length decreases simultaneously, due to the implicit increase of the normalized attenuation[6].

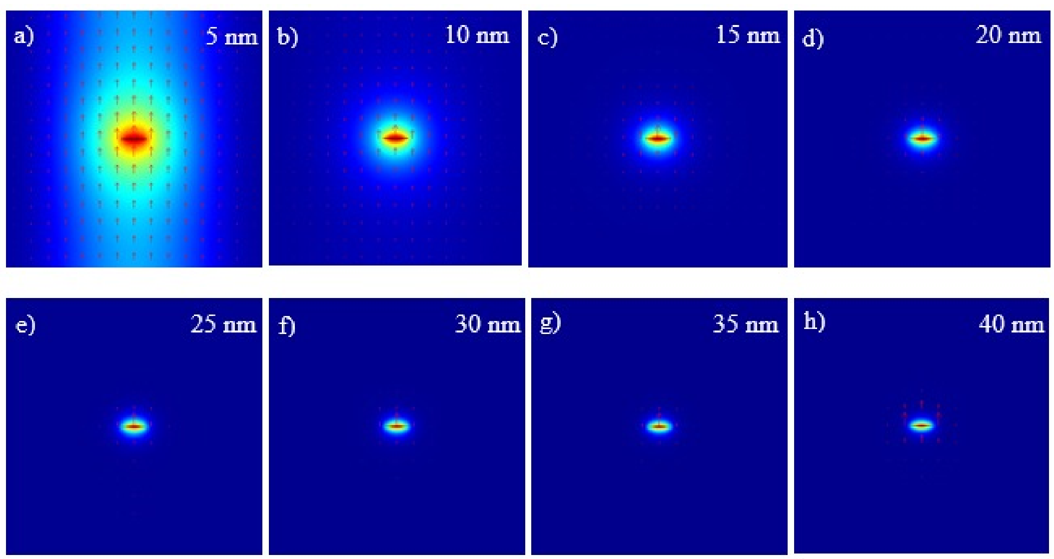


Figure 3. Propagating modes for different metal thicknesses.

Table 1 shows the calculated effective index of refraction for a plasmon mode in a symmetrical structure. It is observed that by increasing the thickness of the gold layer, the normalized attenuation increases simultaneously, therefore, the propagating wave length decreases[6]. In Fig. 4, a plot of the effective refraction index as a function of the metal layer thickness is shown.

Table 1. Real and imaginary parts of the effective index of refraction for different metal thicknesses.

| VARIABLE THICKNESS | | |
|---|---|---|
| t (nm) | neff | keff ($X10^{-6}$) |
| 5 | 1.339929 | 0.0487 |
| 10 | 1.339969 | 0.3652 |
| 15 | 1.340066 | 2.3974 |
| 20 | 1.340286 | 10.4206 |
| 25 | 1.340648 | 28.8434 |
| 30 | 1.341113 | 59.7472 |
| 35 | 1.341621 | 103.0133 |
| 40 | 1.342123 | 156.6412 |

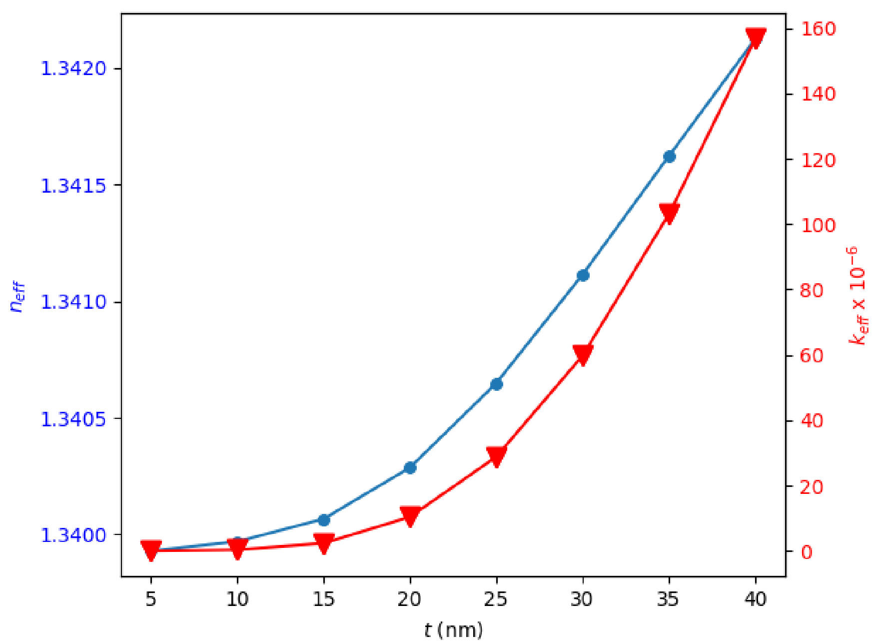


Figure 4. Real part ($n_{eff}$) and imaginary part ($k_{eff}$) of the effective refractive index of the optical supported by the plasmonic waveguide, as a function of the thickness layer ($t$) for an Au layer embedded in Cytop.

For a metal thickness of 30 nm, the effective refraction index was calculated by varying the refraction index of the upper box of the geometry shown in Fig 2. The results are presented in Table 2, these results show that the normalized attenuation is lower as the difference between the refractive index of Cytop and that of the analyte decreases i.e., attenuation decreases with claddings that more optically symmetric. However, the as the difference in refractive index increases the propagating modes are less symmetric "electromagnetic wave is scattered through the layer of greater refractive index[10].

Table 2. Real and imaginary parts of the effective index of refraction for varying $n_3$.

| ANALYTE REFRACTIVE INDEX | | |
|---|---|---|
| n Analyte | $n_{eff}$ | $k_{eff}$ (x$10^{-6}$) |
| 1.3300 | 1.339452 | 18.9832 |
| 1.3305 | 1.339458 | 19.5901 |
| 1.3310 | 1.339466 | 20.3099 |
| 1.3315 | 1.339475 | 21.1724 |
| 1.3320 | 1.339485 | 22.2178 |
| 1.3325 | 1.339497 | 23.5010 |
| 1.3330 | 1.339511 | 25.0978 |
| 1.3335 | 1.339528 | 27.1128 |
| 1.3340 | 1.339549 | 29.6889 |
| 1.3345 | 1.339576 | 33.0117 |
| 1.3350 | 1.339612 | 37.2922 |
| 1.3355 | 1.339659 | 42.6780 |
| 1.3360 | 1.339724 | 49.0186 |
| 1.3365 | 1.339811 | 55.5103 |
| 1.3370 | 1.339928 | 60.6796 |
| 1.3375 | 1.340075 | 63.2644 |
| 1.3380 | 1.340250 | 63.2184 |
| 1.3385 | 1.340449 | 61.5504 |
| 1.3390 | 1.340666 | 59.4813 |
| 1.3395 | 1.340898 | 57.9254 |
| 1.3400 | 1.341144 | 57.3938 |

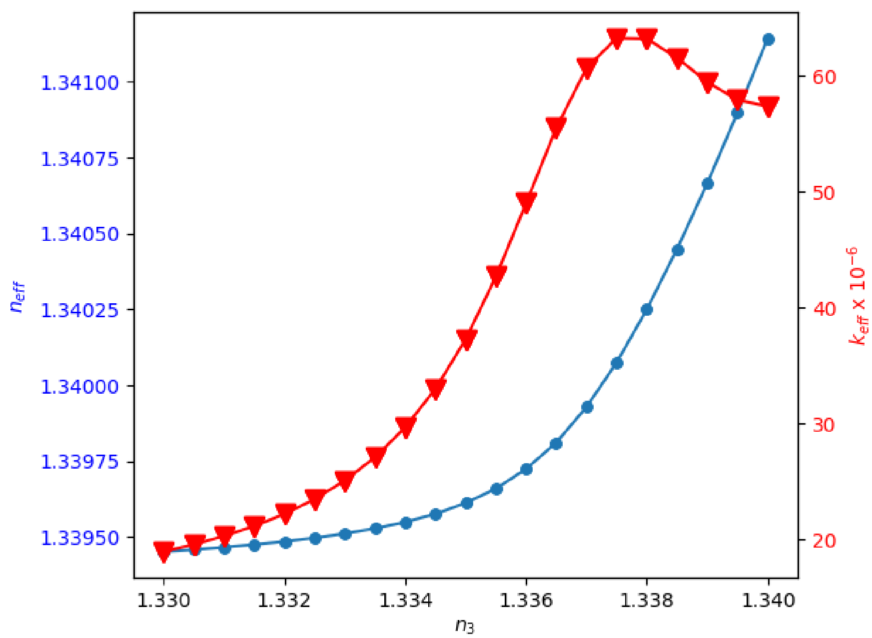


Figure 5. The behavior of complex effective index $N_{eff} = n_{eff} + j\, k_{eff}$ as a function of surface detection refractive index $n_3$.

## 4. FINAL REMARKS

We performed a parametric study for a LRSPP device consisting of a plasmonic waveguide whose claddings have refractive index around that of water. The effective complex refractive index of the supported optical mode was calculated as a function of the thickness of the metal film. It was shown that the confinement decreases while the losses monotonically increases as the metal layer thickness decreases. In order to assess the potential use of such plasmonic waveguide as a biosensor, we evaluated the changes in the effective refractive index with respect to the changes in the refractive index of the analyte. We demonstrated that the device can, in fact, be used to identify minimal differences between the upper and bottom claddings and therefore can be potentially used as a high-sensitivity sensor. Finally, since the index mismatch between the claddings greatly impacts both the real and the imaginary part of the effective complex refractive index if the supported mode, in such a geometrical arrangement the interrogation scheme can be implemented either in terms of the accumulated phase or the attenuation thanks to the millimeter-length propagation distance which is characteristic of a LRSPP-based devices.

## REFERENCES


[1] Thévenot, D. R., Toth, K., Durst, R. A. and Wilson, G. S., "Electrochemical biosensors: Recommended definitions and classification," Biosens. Bioelectron. **16**(1–2), 121–131 (2001).

[2] Arghir, I., Delport, F., Spasic, D. and Lammertyn, J., "Smart design of fiber optic surfaces for improved plasmonic biosensing," N. Biotechnol. **32**(5), 473–484 (2015).

[3] Krupin, O., Wong, W. R., Beland, P., Mahamd Adikan, F. R. and Berini, P., "Long-range surface plasmon-polariton waveguide biosensors for disease detection," J. Light. Technol. **34**(20), 4673–4681 (2016).

[4] Zayats, a, Smolyaninov, I. and Maradudin, a., "Nano-optics of surface plasmon polaritons," Phys. Rep. **408**(3–4), 131–314 (2005).

[5] Maier, S. A., [Plasmonics: Fundamentals and applications] (2007).

[6] Berini, P., "Long-range surface plasmon polaritons," Adv. Opt. Photonics **1**(3), 484 (2009).

[7] Liedberg, B., Nylander, C. and Lunström, I., "Surface plasmon resonance for gas detection and biosensing," Sensors and Actuators **4**(C), 299–304 (1983).

[8] Hammond, J. L., Formisano, N., Estrela, P., Carrara, S. and Tkac, J., "Electrochemical biosensors and nanobiosensors," Essays Biochem. **60**(1), 69–80 (2016).

[9] Khodami, M. and Berini, P., "Biomolecular kinetics analysis using long-range surface plasmon waveguides," Sensors Actuators, B Chem. (2017).

[10] Krupin, O., Wong, W. R., Mahamd Adikan, F. R. and Berini, P., "Detection of Small Molecules Using Long-Range Surface Plasmon Polariton Waveguides," IEEE J. Sel. Top. Quantum Electron. **23**(2) (2017).

[11] Krupin, O., Khodami, M., Fan, H., Wong, W. R., Mahamd Adikan, F. R. and Berini, P., "Biosensing using long-range surface plasmon waveguides," Proc. SPIE - Int. Soc. Opt. Eng. **10242**(May 2017), 1–7 (2017).

[12] Khanarian, G. and Celanese, H., "Optical properties of cyclic olefin copolymers," Opt. Eng. (2001).

[13] Leosson, K. and Agnarsson, B., "Integrated biophotonics with CYTOP," Micromachines **3**(1), 114–125 (2012).

[14] Filion-Côté, S., Tabrizian, M. and Kirk, A. G., "Real-time measurement of complex refractive indices with surface plasmon resonance," Sensors Actuators, B Chem. (2017).

[15] Lee, S. and Kim, S., "Long-range channel plasmon polaritons in thin metal film V-grooves," Opt. Express **19**(10), 9836 (2011).